

Impact of Layer Orientation on Radio Frequency Dielectric Properties of Fused Filament Fabricated ULTEM 9085

Carson Rogers¹, Jutima Simsiriwong¹, Juan Aceros¹, and Daniel Santavicca²

¹School of Engineering, University of North Florida, Jacksonville, FL 32224

²Department of Physics, University of North Florida, Jacksonville, FL 32224

Abstract

ULTEM 9085 is a thermoplastic material commonly used in high performance fused filament fabricated (FFF) parts and has been selected as a material of interest for use in L, S, and X band naval radome applications due to its excellent mechanical and thermal properties. However, previous studies have found that the FFF process induces anisotropic effects in the electromagnetic transmissivity of parts manufactured with this process due to the layering of the filament. In this study, the effects of layer orientation on the dielectric properties of FFF ULTEM 9085 specimens are investigated using a rectangular waveguide from 9 to 15 GHz. This is outside the range of frequencies previously reported. The resultant dielectric properties are discussed in relation to the layer orientation of the specimens.

Keywords: ULTEM 9085, Fused Filament Fabrication, Radome, Dielectric Properties, Layer Orientation

Introduction

Additive manufacturing (AM) processes, such as fused filament fabrication (FFF) offer many advantages compared to traditional subtractive manufacturing processes. Some of these advantages include the ability to create complex solid parts, and decreased manufacturing times and waste production. The FFF process is an AM process that involves passing a continuous filament through a heated nozzle, also known as a liquefier, and depositing the melt on a build platform [1]. Once a completed layer of material is deposited, the nozzle indexes vertically to begin depositing a second layer, and so on. A graphic of the FFF process can be found in Figure 1. Additionally, AM processes, particularly FFF, offer a streamlined pathway for repair and rework through the existing workflow of 3D scanning that captures a detailed profile of the damaged parts. In this work, the FFF process is being explored in naval applications to fabricate/repair parts onsite, thus reducing supply chain lead times and associated costs.

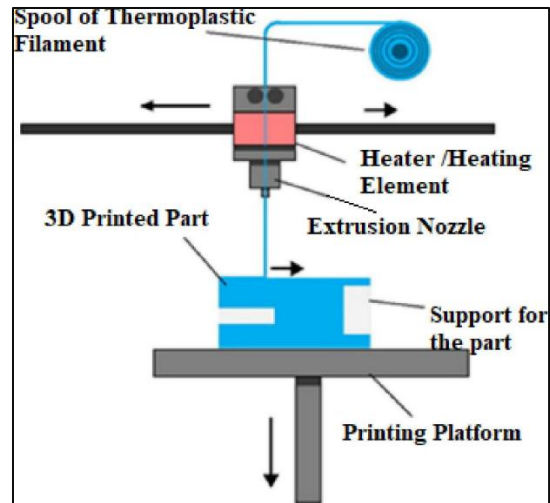


Figure 1: Fused filament fabrication process [3].

ULTEM 9085 is a high-performance thermoplastic used in injection molding and FFF manufacturing processes. ULTEM 9085 is a blend of polyetherimide and polycarbonate, and [2]. ULTEM 9085 is known for its excellent mechanical properties, chemical resistance, and thermal stability [2,4]. Due to its advanced properties, ULTEM 9085 has been selected as a material of interest for use in naval radome repair applications. Other materials such as acrylonitrile styrene acrylate (ASA) were initially considered as materials of interest. ASA is known for its resistance to UV radiation and heat fluctuations. Both UV resistance and thermal resistance are important factors for parts exposed to the outside environment. However, ASA does not compare to ULTEM 9085 mechanically. ULTEM 9085 exhibits a yield strength more than twice that of ASA (69.2 MPa) and has a significantly higher modulus of elasticity [4].

A radome is a protective structure used to shield sensitive communications equipment. For naval radome applications, the constructive material must be mechanically strong so that the structure does not fail due to bird strikes, strong winds, or hail. It must also be resistant to environmental effects such as high humidity, salinity, temperature fluctuations, and intense amounts of ultraviolet radiation. One of the most important factors in selecting a material for radome applications is its transmissivity to the frequencies of interest. The incoming radiation must be able to pass through the radome so that the enclosed equipment can receive the signal. Although the FFF process offers quick production times, it does have the downside of intrinsic anisotropy, which is induced by the layering of the material in the FFF process [6]. These anisotropic effects are most commonly noticed in the mechanical performance of materials, where tensile failure often initiates on the planes parallel to the layered filament which are orthogonal to the applied load [7]. However, the layering of material in the FFF process has also been found to influence dielectric properties [4].

The anisotropic effects of the FFF process on the dielectric properties of Ultem 9085 in radio frequencies have largely been uncharacterized. Therefore, the scope of this study is to

determine the dielectric constant, loss tangent, and electromagnetic transmissivity of ULTEM 9085 parts manufactured in each layer orientation. The performance of each specimen will be assessed through the use of a WR-75 waveguide resonator, which supports a fundamental TE transmission mode from approximately 9 to 15 GHz, which is measured with a vector network analyzer (VNA). The results of this study will provide a relationship between print orientation and dielectric performance in the X-band frequencies for parts made of ULTEM 9085.

Some mechanical, thermal, and dielectric properties of ULTEM 9085 properties have been reported by Stratasys, as tabulated in Tables 1 and 2. Regarding the dielectric properties, tests were conducted following ASTM D150 at 1 kHz and 2 MHz to obtain the dielectric constant and the loss tangent. The dielectric constant can be defined as the ratio between the capacitance of a dielectric in a plate capacitor to the capacitance of an open plate capacitor. The loss tangent is a measure of the energy loss of a signal as it passes through a dielectric material. While the reported dielectric properties of Ultem 9085 are outside of the range of radio frequencies, anisotropy is still evident, with XY-oriented specimens exhibiting lower dielectric constants compared to YZ/ZX-oriented specimens.

Table 1: Mechanical and thermal properties of ULTEM 9085 [4].

Property	Units	Layer Orientation	
		XY	YZ ¹ /ZX
Modulus of elasticity	GPa	2.52	2.41
Yield Strength	MPa	69.2	N/A
Elongation at Yield	%	5.4	N/A
Strength at Fracture	MPa	68.1	39.4
Elongation at Fracture	%	5.4	1.9
Heat Def. Temp. (66 psi)	°C	176.9	
Glass Transition Temp.	°C	177.32	

Table 2: Dielectric properties of ULTEM 9085 [4].

Property	Frequency	Layer Orientation	
		XY	YZ ¹ /ZX
Dielectric constant	1 kHz	2.80	2.87
	2 MHz	2.65	2.73
Loss tangent	1 kHz	0.002	0.002
	2 MHz	0.010	0.010

¹ Stratasys measured values in the XZ orientation instead of the YZ [4]. However, due to the raster angle used the XZ and YZ layer orientations should produce identical samples.

Other materials such as acrylonitrile styrene acrylate (ASA) were initially considered as materials of interest. ASA is known for its resistance to UV radiation and heat fluctuations. However, ASA does not compare to ULTEM 9085 mechanically. ASA was found to have a tensile yield strength of 32.92 MPa and a modulus of elasticity of 1.74 GPa [5]. ULTEM 9085 was found to yield at a strength over 2 times that of ASA (69.2 MPa). ULTEM 9085 was also found to have a much higher modulus of elasticity of 2.52 GPa in the XY compared to ASA's 1.74 GPa [4].

Although the FFF process offers quick production times and strong parts, it does have the downside of intrinsic anisotropy. The anisotropy is induced by the layering of the material in the FFF process [6]. These anisotropic effects are most commonly noticed in the mechanical performance of materials, where tensile failure often initiates on the planes parallel to the layered filament which are orthogonal to the applied load [7]. However, the layering of material in the FFF process has also been found to influence dielectric properties [4]. The layering of material is defined as the layer orientation and can occur in three configurations: XY, YZ, and ZX. In the XY layer orientation, the stacked layers of material are parallel to the XY plane when the specimen is placed in the waveguide. Similarly, in the YZ orientation, the stacked layers are parallel to the YZ plane, and in the ZX orientation, the stacked layers are parallel to the ZX plane. This means that in the TE transmission mode used by the waveguide, the electric field lines are perpendicular to the material layers of XY specimens, and parallel to the material layers of the YZ and ZX specimens. A visual representation of the three different layer orientations can be viewed in Figure 2..

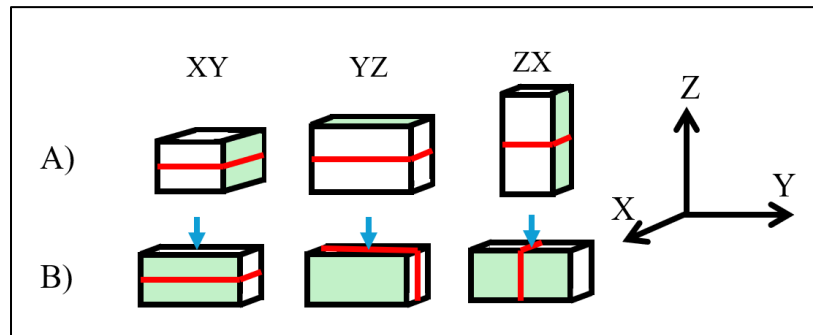


Figure 2: (A) The three layer orientations as printed in the Fortus 450mc. (B) The three layer orientations as seen in the waveguide. The blue arrow indicates the direction of the electric field lines in the waveguide. The red plane indicates the orientation of the material layers.

Experimental Methods

To assess the effects of layer orientation on the dielectric properties of ULTEM 9085 parts, specimens were manufactured using a Stratasys Fortus 450mc FFF 3D printer with Stratasys ULTEM 9085 filament. The specimen geometries were designed to tightly fit into the WR-75

waveguide opening (9.525 mm x 19.05 mm). Nine rectangular samples were produced with dimensions of 9.525 mm x 12.7 mm x 19.05 mm, with three samples of each orientation (XY, YZ, and ZX). All specimens were manufactured with a $\pm 45^\circ$ raster angle and a 100% infill density. No post-processing was conducted on the specimens produced. The specimens were printed with a T16 nozzle (0.254 mm layer height).

Each specimen was placed in a section of WR-75 rectangular waveguide with a length of 88.8 mm. Homemade inductive apertures were placed at each end of the waveguide. The apertures, machined from 2.0 mm thick aluminum, have an opening width of 5.2 mm and height of 9.5 mm. The other side of each aperture was connected to an SMA-to-waveguide adapter (Pasternack PE9819). When a signal is sent through this test setup, partial reflections are generated by each aperture, forming a resonant cavity inside the waveguide. Maxima in the transmission coefficient occur when the length of the resonant cavity is equal to an integer multiple of half the signal wavelength. The test setup can be seen in Figures 3 and 4.

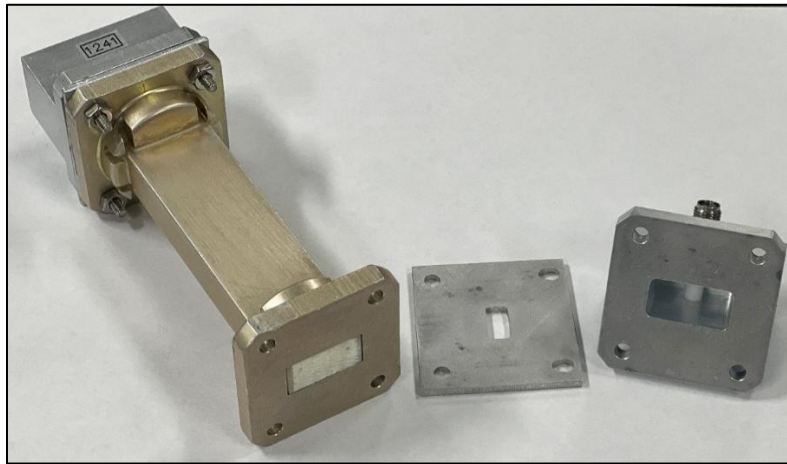


Figure 3: WR-75 waveguide with specimen inserted, inductive aperture, and waveguide port as seen from left to right.

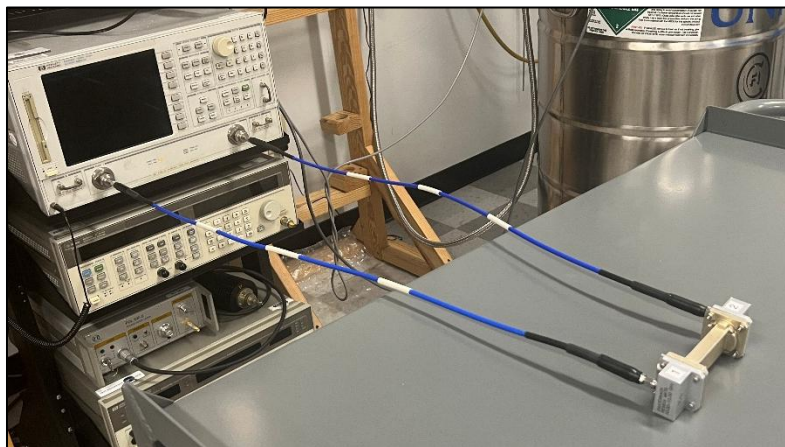


Figure 4: Waveguide setup connected to HP 8720D network analyzer.

The transmission coefficient was measured from 9 to 15 GHz using an HP 8720D vector network analyzer. The measured data were compared to a model in AWR Microwave Office. First, the model was matched to data measured with an empty waveguide. Then, keeping the model parameters for the waveguide and apertures fixed, the model was matched to data measured with each specimen in the waveguide using only the specimen dielectric constant and loss tangent as adjustable parameters. The transmission coefficient is most sensitive to the specimen properties at each resonant frequency, so the matching of the simulation to the data was separately optimized at each of the five resonant frequencies within the measurement bandwidth in order to determine the dielectric constant and loss tangent of the specimen at each resonant frequency. This process was repeated for three different specimens for each layer orientation.

An example of the measured and simulated data from one of the XY specimens are shown in Figures 5 and 6. The y-axis is the magnitude of the transmission coefficient expressed in log units, which is defined as $S_{21} = 10\log(P_{out}/P_{in})$, where P_{in} is the power sent into the waveguide resonator and P_{out} is the power measured at the output. In matching the model to the measured data, the dielectric constant of the specimen is adjusted in the model to best match the resonant frequency and the loss tangent of the specimen is adjusted in the model to best match the height of the resonance peak.

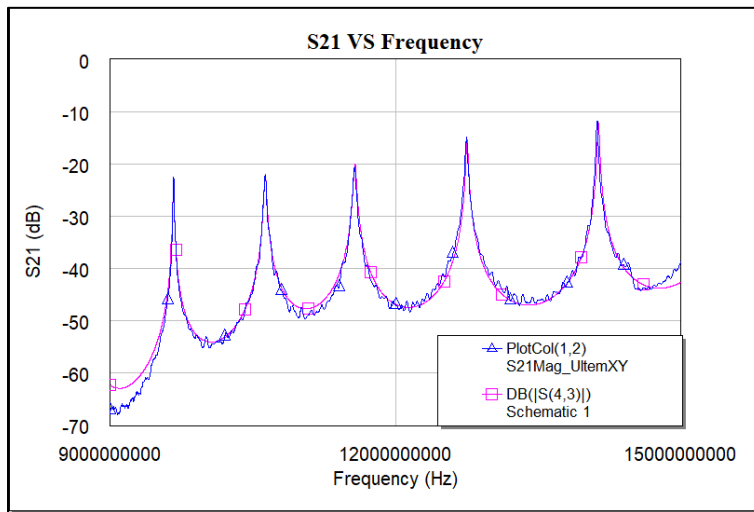


Figure 5: Measured (blue) and simulated (pink) magnitude of the transmission coefficient S_{21} as a function of frequency for the waveguide resonator containing an ULTEM 9085 specimen printed in the XY orientation.

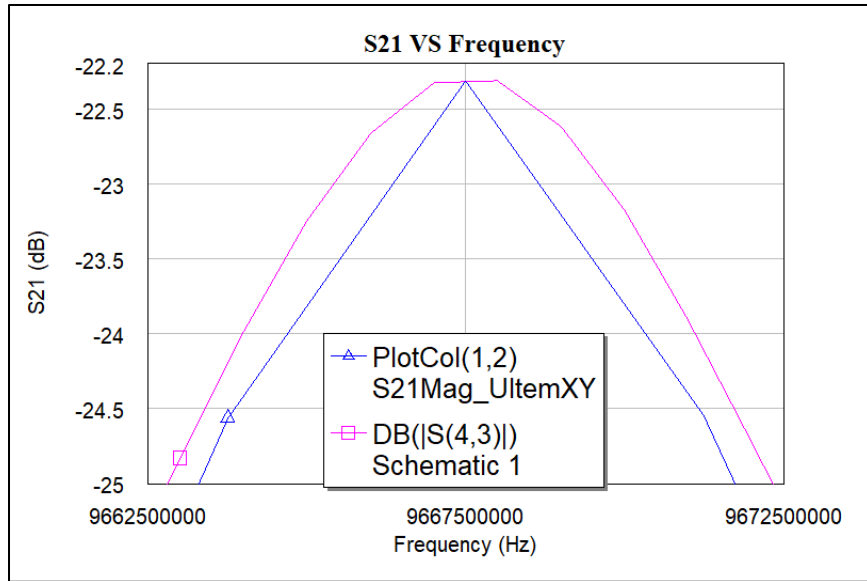


Figure 6: Matching simulated (pink) to the measured (blue) transmission coefficient magnitude S_{21} at one resonance frequency.

Results and Discussions

The dielectric constant and loss tangent were recorded at each resonant peak of every specimen. For each frequency, the results from the three specimens of the same layer orientation were used to calculate an average and a standard error. These results for each orientation can be found in Table 3.

Table 3: Experimental dielectric properties.

Orientation	Resonant Frequency (GHz)	Dielectric Constant	DC Std. Err.	Loss Tangent	LT Std. Err.
XY	9.6653	2.8273	0.0097	0.008187	0.0010
	10.6327	2.8143	0.0032	0.007037	0.0004
	11.5727	2.8187	0.0024	0.007467	0.0004
	12.7453	2.8320	0.0044	0.007253	0.0008
	14.1190	2.8557	0.0062	0.006790	0.0004
YZ	9.6550	2.8963	0.0043	0.008357	0.0003
	10.6063	2.8910	0.0139	0.006673	0.0004
	11.5413	2.8937	0.0116	0.007310	0.0003
	12.7283	2.8870	0.0026	0.007897	0.0007
	14.1060	2.8980	0.0184	0.009007	0.0020
ZX	9.6537	2.8953	0.0273	0.012887	0.0024
	10.5940	2.8953	0.0416	0.007939	0.0007
	11.5333	2.8913	0.0304	0.008417	0.0010
	12.7303	2.8747	0.0142	0.010551	0.0015
	14.1127	2.8803	0.0185	0.008655	0.0012

A graphical representation of the dielectric constants plotted against frequency can be seen in Figure 8. Across the entire range of interest, the XY orientation specimens produced the lowest dielectric constants, while the YZ and ZX orientations produced similar dielectric constants. On average, the dielectric constant of the specimens printed in the XY layer orientation (2.8296) was 2.2% lower than those printed in the YZ layer orientation (2.8932), and 2.0% lower than those printed in the ZX layer orientation (2.8874).

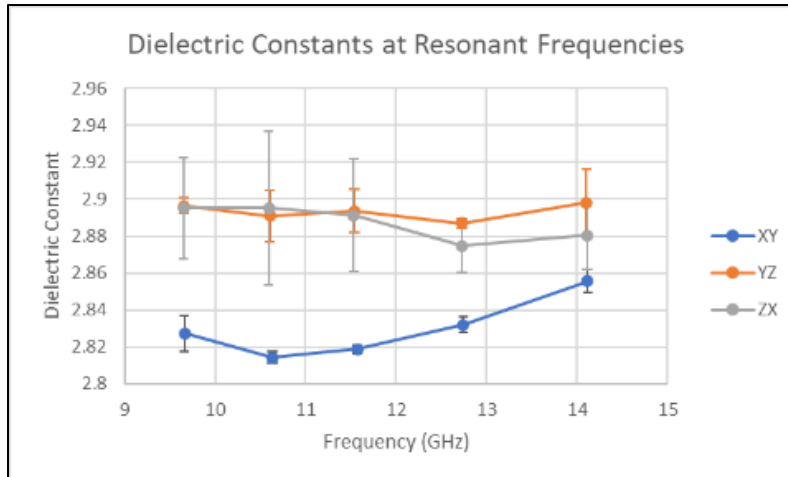


Figure 8: The dielectric constants of each orientation at their respective resonant frequencies. The error bars show the standard error.

In addition to the dielectric constant, the loss tangent was also assessed based on the resonant frequency. A graphical representation of the loss tangent with respect to resonant frequency and layer orientation can be seen in Figure 9. The specimens printed in the ZX layer orientation were found to produce higher loss tangents compared to those printed in the XY and YZ layer orientations. On average, the loss tangents produced by specimens printed in the ZX orientation (.0097) were 24.2% higher than those printed in the XY layer orientation (.0073) and 19.0% higher than those printed in the YZ layer orientation (.0078). However, the standard error of the loss tangent for each layer orientation at each resonant frequency is relatively high. This means that the recorded relationship between layer orientation and the loss tangent could be different in reality. At each resonant frequency, the error bars (standard error) of two or all of the layer orientations intersect.

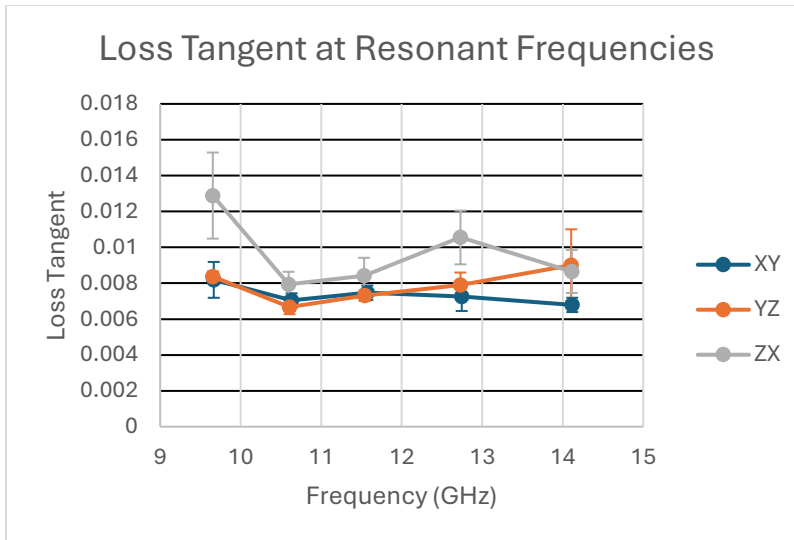


Figure 9: The loss tangent of each orientation at their respective resonant frequencies. The error bars show the standard error.

The directionality of the measured dielectric constants and loss tangents is likely due to void alignment within each specimen. Most voids that form during FFF processes are formed in planes parallel to the material layers. These voids include raster gap voids, partial neck growth voids, and inter-bead voids [8]. This implies that the voids form directionally based on the layer orientation of the printed part. This also explains the similar performance of the YZ and ZX layer orientations regarding the dielectric constant. The voids in the specimens printed in the YZ and ZX layer orientations are aligned parallel to the applied electric field in the waveguide. The specimens printed in the XY layer orientation contain voids that are aligned perpendicularly to the applied electric field in the waveguide. This alignment of voids means that the electric field interacts with the combined dielectric effects of the voids (trapped air) and ULTEM 9085 differently with the specimens printed in the XY layer orientation compared to those in the YZ and ZX layer orientations. The alignment of voids can be visualized by the red planes in Figure 2, where the red plane is perpendicular to the applied electric field in the XY layer orientation, and parallel to the electric field in the YZ and ZX layer orientations.

The ULTEM 9085 specimens were found to contain similar dielectric properties to common radome materials such as silica/epoxy composites. One study found that a silica/epoxy composite radome material achieved a dielectric constant of 3.95 and a loss tangent of 0.045 [9]. The ULTEM 9085 specimens were found to have similar dielectric properties. The average dielectric constant of all ULTEM 9085 samples was 2.87, and the average loss tangent was 0.0083.

Conclusions

The objective of this study was to investigate the effects of layer orientation on the dielectric properties of FFF parts manufactured with ULTEM 9085 from 9 to 15 GHz. Previously, the relationship between dielectric properties and layer orientation had been reported at 1 kHz and 2 MHz [4]. The experimental results in this study reveal that the XY specimens produces a lower dielectric constant across the frequency range of interest compared to the specimens built in YZ and ZX orientations. The YZ and ZX specimens exhibit approximately the same dielectric constants. The resulting loss tangent indicates minimal layer orientation dependence, which is similar to those obtained previously [4].

The layer orientation dependence on the dielectric constant is likely explained by the alignment of internal voids in the samples. The voids formed in the specimens printed in the XY layer orientation appear in planes perpendicular to the applied electric field in the waveguide. In contrast, the voids formed in the specimens printed in the YZ and ZX layer orientations appear in planes parallel to the applied electric field. The variation in interactions between the material and the applied electric field suggests that the combined effects of voids and the ULTEM 9085 may result in orientation-dependent dielectric properties. Future testing on ULTEM 9085 will assess the void density of each specimen and evaluate the extent to which void orientation depends on the specimen's layer orientation.

Comparing the resultant dielectric properties of the ULTEM 9085 samples to those of common radome materials such as silica/epoxy composites, ULTEM 9085 produces similar properties [9]. This indicates that ULTEM 9085 has the potential to be an effective radome material.

Acknowledgement

This research is based on the work funded by the Naval Engineering Education Consortium (NEEC).

References

- [1] A. R. Zanjanijam et al, "Fused Filament Fabrication of PEEK: A Review of Process-Structure-Property Relationships," *Polymers*, vol. 12, (8), 2020.
- [2] X. Wang, C. Travis, M. Sorna, and D. Arola, "Durability of ULTEM 9085 in Marine Environments: A consideration in fused filament fabrication of structural components," *Polymers*, vol. 16, no. 3, p. 350, Jan. 2024. doi:10.3390/polym16030350
- [3] A. Jaisingh Sheoran and H. Kumar, "Fused deposition modeling process parameters optimization and effect on mechanical properties and part quality: Review and reflection on present research," *Materials Today: Proceedings*, vol. 21, pp. 1659–1672, 2020. doi:10.1016/j.matpr.2019.11.296
- [4] "ULTEMTM 9085 resin: High performance thermoplastic," ULTEMTM 9085 resin: High Performance Thermoplastic, <https://www.stratasys.com/en/materials/materials-catalog/fdm-materials/ULTEM-9085/>.
- [5] W. Cahyadi, "Mechanical Properties of 3D Printed Acrylonitrile Styrene Acrylate," South Dakota State University, master's thesis, May 2019, available at <https://openprairie.sdstate.edu/etd/3187/>
- [6] T. Q. Tran et al, "Tensile Strength Enhancement of Fused Filament Fabrication Printed Parts: A Review of Process Improvement Approaches and Respective Impact," *Additive Manufacturing*, vol. 54, 2022.
- [7] A. Garg and A. Bhattacharya, "An insight to the failure of FDM parts under tensile loading: Finite Element Analysis and experimental study," *International Journal of Mechanical Sciences*, vol. 120, pp. 225–236, Jan. 2017. doi:10.1016/j.ijmecsci.2016.11.032
- [8] Y. Tao et al., "A review on voids of 3D printed parts by fused filament fabrication," *Journal of Materials Research and Technology*, vol. 15, pp. 4860–4879, Nov. 2021. doi:10.1016/j.jmrt.2021.10.108
- [9] I. Haider, I. H. Gul, M. M. Baig, and M. A. Umer, "Dielectric and thermal properties of composite radome material under Accelerated Aging: An Experimental Study," *Journal of Materials Science: Materials in Electronics*, vol. 35, no. 7, Mar. 2024. doi:10.1007/s10854-024-12098-2

Appendix

A1: Measured dielectric constant and loss tangent at their associated resonant frequencies.

Orientation (Sample)	Resonant Frequency (GHz)	Dielectric Constant	Loss Tangent
XY (1)	9.668	2.808	0.00640
	10.628	2.809	0.00654
	11.569	2.814	0.00687
	12.746	2.824	0.00573
	14.121	2.849	0.00616
XY (2)	9.664	2.838	0.01002
	10.639	2.820	0.00782
	11.580	2.820	0.00826
	12.748	2.833	0.00798
	14.121	2.850	0.00675
XY (3)	9.664	2.836	0.00814
	10.631	2.814	0.00675
	11.569	2.822	0.00727
	12.742	2.839	0.00805
	14.115	2.868	0.00746
YZ (1)	9.653	2.899	0.00832
	10.598	2.891	0.00608
	11.535	2.891	0.00720
	12.728	2.883	0.00700
	14.110	2.887	0.00710
YZ (2)	9.656	2.902	0.00793
	10.605	2.915	0.00648
	11.539	2.915	0.00684
	12.731	2.886	0.00918
	14.112	2.873	0.00688
YZ (3)	9.656	2.888	0.00882
	10.616	2.867	0.00746
	11.550	2.875	0.00789
	12.726	2.892	0.00751
	14.096	2.934	0.01304
ZX (1)	9.656	2.868	0.00816
	10.613	2.835	0.00661
	11.546	2.848	0.00690

	12.728	2.873	0.00842
	14.104	2.911	0.00890
ZX (2)	9.641	2.950	0.01548
	10.549	2.975	0.00875
	11.498	2.950	0.01019
	12.720	2.900	0.00977
	14.111	2.883	0.01052
ZX (3)	9.664	2.868	0.01502
	10.620	2.876	0.00846
	11.556	2.876	0.00816
	12.743	2.851	0.01346
	14.123	2.847	0.00655